

## New opportunities in the study of in-medium nuclear properties with FAZIA

DIEGO GRUYER<sup>(1)</sup>(\*) and JOHN D. FRANKLAND<sup>(2)</sup>

<sup>(1)</sup> INFN, Sezione di Firenze - via Sansone 1, I-50019 Sesto Fiorentino (FI), Italy

<sup>(2)</sup> Grand Accélérateur National d'Ions Lourds (GANIL), CEA/DRF-CNRS/IN2P3  
Bvd. Henri Becquerel, 14076 Caen, France

received 10 January 2017

**Summary.** — In this contribution we investigate the capabilities (resolution and efficiency) of the FAZIA demonstrator, with a particular emphasis on light cluster structure studies (excited state energy, width, and spin) and emitting source characterization (temperature and density), using multi-particle correlations. This study has been performed on simulated  $^{32}\text{S} + ^{12}\text{C}$  collisions from 25 to 80 MeV/A.

### 1. – Introduction

The nuclear matter equation of state (EoS) is an essential ingredient in the description of core-collapse supernovae dynamics and structure of the neutron star crusts [1]. Huge efforts are made to improve our knowledge of the nuclear EoS, especially for asymmetric nuclear matter where the lack of experimental data leads to large discrepancies between different predictions [2]. In addition, at densities below nuclear saturation density, clusters appear and the chemical composition of nuclear matter is modified which strongly affect its thermodynamical properties [3]. Recent theoretical studies suggest that nuclear matter clusterization may play a more important role than symmetry energy in accreting neutron-star crusts [4]. The main challenges of our discipline can be summarized by three questions:

- 1) What is the equation of state of asymmetric nuclear matter?
- 2) How does nuclear matter clusterize at low density?
- 3) How do clusters behave in low density nuclear medium?

(\*) E-mail: diego.gruyer@fi.infn.it



Fig. 1. – INDRA-FAZIA coupling: the FAZIA demonstrator in the INDRA scattering chamber (left); the FAZIA demonstrator geometry considered in this contribution (right).

Heavy-ion collisions at intermediate energy offer a unique possibility to constrain the nuclear EoS and to study the effects of correlations and the modification of cluster properties in dilute matter [5, 6]. In this energy regime, violent heavy-ion collisions produce many particles over a large range of charge ( $Z$ ), mass ( $A$ ) and kinetic energy ( $E_k$ ). Studying this kind of reactions requires detectors with almost  $4\pi$ -solid-angle coverage, high granularity, low-energy thresholds, large dynamic range in energy and capable of characterizing reaction products on an event by event basis. The first generation of  $4\pi$  multi-detectors focused on complete collection of charged particles produced in a reaction [7-11], providing little isotopic information for heavy fragments ( $Z > 5$ ).

More recently detectors have evolved to provide isotopic resolution for a broader range of products [12, 13], by improving existing identification techniques, or developing new method such as the Pulse Shape Analysis (PSA) in silicon detectors [14-16]. Among these new detectors, the future coupling of the FAZIA [13] demonstrator with the backward part of INDRA will provide a very efficient tool at GANIL for investigating in-medium nuclear properties and nuclear EoS in extreme conditions.

In this contribution we estimate the resolution and efficiency of the FAZIA demonstrator for multi-particle correlations studies. This study was performed on simulated  $^{32}\text{S} + ^{12}\text{C}$  collisions from 25 to 80 MeV/A.

## 2. – The future INDRA-FAZIA coupling at GANIL

The INDRA multidetector [8], in operation at GANIL since 1993, is currently composed of 336 detection cells arranged in 17 rings centered on the beam axis and covers 90% of the solid angle. The first ring ( $2^\circ$  to  $3^\circ$ ) is made of 12 telescopes composed of  $300\ \mu\text{m}$  silicon wafers (Si) and CsI(Tl) scintillators (14 cm thick). Rings 2 to 9 ( $3^\circ$  to  $45^\circ$ ) are composed of 12 or 24 three-member detection telescopes: a 5 cm thick ionization chamber (IC) with  $2.5\ \mu\text{m}$  Mylar windows operated with 20 mbar of  $\text{C}_3\text{F}_8$  gas; a 300- or  $150\text{-}\mu\text{m}$  silicon wafer; and a CsI(Tl) scintillator (14 to 10 cm thick) coupled to a photomultiplier tube. Rings 10 to 17 ( $45^\circ$  to  $176^\circ$ ) are composed of 24, 16, or 8 two-member telescopes: an ionization chamber and a CsI(Tl) scintillator of 8, 6, or 5 cm thickness. This apparatus allows to identify in charge fragments from hydrogen to uranium with low thresholds. The mass identification is however limited to particles crossing the silicon layer and with a charge lower than 6.

In the near future, the first 5 rings of INDRA ( $2^\circ$  to  $14^\circ$ ) should be replaced by the FAZIA demonstrator composed of 12 FAZIA blocks in wall configuration (see fig. 1),

placed 1 metre downstream of the target to cover polar angles from  $2^\circ$  to  $13^\circ$ . A FAZIA block is made of 16 Si(300  $\mu\text{m}$ )-Si(500  $\mu\text{m}$ )-CsI(Tl)(10 cm) telescopes covering a surface of  $2 \times 2 \text{ cm}^2$  and mounted in a square geometry. Each silicon detector is of the neutron transmutation doped type (n-TD) and reverse mounted (*i.e.* with particles impinging on the low electric field side); has a thickness uniformity around 1  $\mu\text{m}$  and a doping uniformity better than 6% of Full Width Half Maximum (FWHM); and is cut at  $7^\circ$  with respect to the  $\langle 100 \rangle$  axis of silicon lattice to avoid channeling. Particles stopped in the first silicon layer are identified by PSA of the current signal while those crossing the first silicon are identified by the  $\Delta E$ - $E$  technique. With such telescopes, we can obtain a charge identification for all detected fragments and isotopic identification up to  $Z \sim 25$  using the  $\Delta E$ - $E$  technique (see fig. 1 of [17]) and up to  $Z \sim 20$  using PSA with an energy threshold depending on the ion charge. Four FAZIA blocks are already in operation at LNS (Catania, Italy) [18, 17]. We focus here on the expected performances of the FAZIA demonstrator.

### 3. – Method

We have considered here the multiparticle decay of  $^{12}\text{C}^*$ ,  $^{12}\text{N}^*$ , and  $^7\text{Li}^*$  produced in the  $^{32}\text{S} + ^{12}\text{C}$  reaction at 25, 35, 50, and 80 MeV/A beam energy. The procedure used to estimate the performances of the FAZIA demonstrator is basically as follows: modellisation of the reaction using HIPSE; simulation of the  $^{12}\text{N}$ ,  $^7\text{Li}$ , and  $^{12}\text{C}$  multiparticle decay; event filtering with a realistic response of the FAZIA demonstrator; and finally extraction of the resolution and efficiency of the apparatus.

**3.1. Phase space generation with HIPSE.** – The collision dynamics has been simulated using HIPSE [19], which is an event generator dedicated to the description of nuclear collisions in the intermediate energy regime. For each system,  $10^6$  collisions have been simulated. Model parameters (hardness of the potential, percentage of exchange, and percentage of nucleon-nucleon collisions) were fixed following the author recommendations.

**3.2. Multiparticle decay.** – We consider here the following decays:

- 1)  $^{12}\text{C}^* \rightarrow 3\alpha$ ,
- 2)  $^{12}\text{N}^* \rightarrow ^{11}\text{C} + p$ ,
- 3)  $^7\text{Li}^* \rightarrow \alpha + t$ .

The decay mode of the  $^{12}\text{C}$  Hoyle state is still debated since measurements performed in direct and fragmentation reactions lead to percentages of  $3\alpha$  direct decay ranging from 0% [20] to 7% [21]. The small energy separation between direct and sequential decay (92 keV) makes it a good candidate to explore in-medium nuclear property modifications.  $^{12}\text{N}$  is also interesting in this view since all excited states are above the proton separation threshold. A wide part of the spectroscopy of this nucleus can be studied using  $^{11}\text{C}-p$  correlations. The  $^7\text{Li}$  decay has been chosen because it is widely used as thermometer in fragmentation reactions.

For each beam energy,  $2 \cdot 10^6$  decays have been generated. The velocity distributions of decaying nuclei have been extracted from the HIPSE calculations. The excitation energy has been taken randomly in the interval  $E^* \in [E_{th} : E_{th} + 10 \text{ MeV}]$ , where  $E_{th}$  is the energy threshold for the considered decay mode. Outgoing particles were randomly oriented in the decaying nucleus' rest frame.

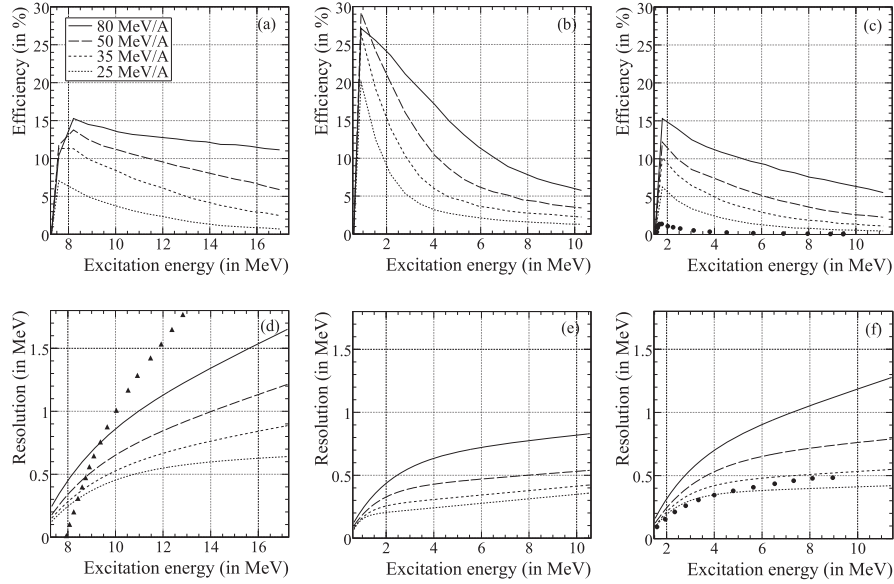


Fig. 2. – Detection efficiency (first row) and FWHM energy resolution (second row) of the FAZIA demonstrator as a function of the excitation energy of the decaying nucleus for:  $^{12}\text{C} \rightarrow 3 \alpha$  decay (first column),  $^{12}\text{N} \rightarrow ^{11}\text{C} + p$  decay (second column),  $^7\text{Li} \rightarrow \alpha + t$  decay (third column). Symbols show efficiency and resolution taken from the literature: resolution of the INDRA detector in the reaction C + Mg at 53 MeV/A [22] (triangles), efficiency and resolution of the hodoscope used in [23] in the reaction Ar + Au at 60 MeV/A (circles).

**3.3. Event filtering.** – Simulated events were then filtered with a realistic response of the setup, using the KaliVeda C++ toolkit [24]. In this work we consider only particles detected in the FAZIA demonstrator (see fig. 1). The first step consists in a geometrical filtering. Cases in which several particles are detected in the same telescope have been removed. The interaction point is taken randomly inside the entrance window of the detector in which the particle has been stopped. Identification energy thresholds are taken from [25]. An energy resolution of 1% FWHM has been considered for all detected particles, which can be considered as an upper limit of the FAZIA energy resolution.

#### 4. – Results

**4.1. Efficiency and resolution.** – Detection efficiency and FWHM energy resolution of the FAZIA demonstrator are shown in fig. 2 for the three decay modes considered here. A few general (and maybe obvious) observations can be made. Efficiency first increases with increasing decaying nucleus excitation energy due to the decrease of pile-up, reaches a maximum and then decreases. Resolution always increases with increasing decaying nucleus excitation energy. The efficiency increases with increasing beam energy and exit channel asymmetry. Resolution increases with increasing beam energy.

Detection efficiency and energy resolution taken from [23] and [22] are also shown in fig. 2(c), (d), (f) for comparison. It should be noted that these numbers were obtained in different reactions and the hodoscope detector was not at the same polar angle. Nevertheless, it can be seen that the resolution obtained with the FAZIA demonstrator is

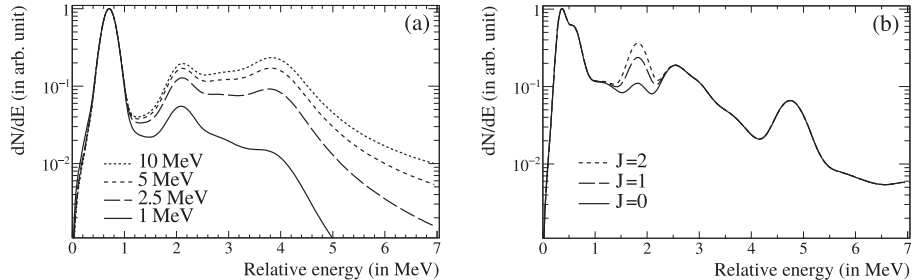


Fig. 3. – Relative energy spectrum calculated from eq. (1) after convolution by the FAZIA demonstrator response in the  $^{32}\text{S} + ^{12}\text{C}$  at 50 MeV/A reaction for (a)  $^{7}\text{Li}^* \rightarrow \alpha + t$  decay with different emission source temperatures ( $T = 1, 2.5, 5, 10$  MeV) and (b)  $^{12}\text{N}^* \rightarrow ^{11}\text{C} + p$  decay with different values of the first  $0^+$  state (2.4 MeV) spin ( $J = 0, 1, 2$ ).

much better than the one obtained with INDRA alone (see fig. 2(d)). The resolution of FAZIA is more similar to the hodoscope one (see fig. 2(f)), while the efficiency of FAZIA is higher by one order of magnitude (see fig. 2(c)).

**4.2. Temperature and spin determination.** – The excitation energy spectrum of a given nucleus produced in heavy-ion collisions can be used to estimate the emitting source temperature [23] and the spin of excited states [26]. Indeed, in the thermal model framework, the excitation energy spectrum can be written as the product of a Maxwellian term and the sum of the individual excited states shape:

$$\frac{dn(E)}{dE} \propto e^{-E/T} \sum_i (2J_i + 1) \frac{\Gamma_i/2\pi}{(E - E_i)^2 + \Gamma_i^2/4},$$

where  $E$  is the excitation energy of a given nucleus produced in an equilibrated source of apparent temperature  $T$ ; and  $E_i$ ,  $\Gamma_i$ , and  $J_i$  are the energy of the centroid, the width, and the spin of the  $i$ -th excited state.

Figure 3(a) presents the  $\alpha$ - $t$  relative energy spectrum calculated from eq. (1) after convolution by the FAZIA demonstrator response for the  $^{7}\text{Li}^*$  decay, using emission source temperature ( $T$ ) ranging from 1 MeV to 10 MeV. It can be seen that energy spectra for different temperatures are clearly distinguishable. They can therefore be used as a thermometer with the FAZIA demonstrator.

Figure 3(b) presents the  $^{11}\text{C}$ - $p$  relative energy spectrum calculated from eq. (1) after convolution by the FAZIA demonstrator response for the  $^{12}\text{N}^*$  decay with different values of the first  $0^+$  state (2.4 MeV) spin ( $J = 0, 1, 2$ ). Once again, different curves can be clearly discriminated, so the FAZIA demonstrator performances could allow excited state spin assignment.

## 5. – Conclusion

In this contribution we have investigated the capabilities (resolution and efficiency) of the FAZIA demonstrator, with a particular emphasis on multi-particle correlations. This study has been performed on the decay of  $^{12}\text{C}^*$ ,  $^{12}\text{N}^*$ , and  $^{7}\text{Li}^*$  produced in  $^{32}\text{S} + ^{12}\text{C}$  collisions from 25 to 80 MeV/A. Detection efficiency and energy resolution have been extracted and compared to the literature. It appears that FAZIA has an energy resolution

comparable to a hodoscope, with a detection efficiency characteristic of a multidetector. The INDRA-FAZIA coupling, designed for fragmentation/vaporisation studies will also allow investigation of nuclear structure via multi-particle correlations.

## REFERENCES

- [1] LATTIMER J. M. and PRAKASH M., *Phys. Rep.*, **442** (2007) 109.
- [2] BAO-AN LI *et al.* (Editors), *Eur. Phys. J. A*, **50** (2014).
- [3] RADUTA AD. *et al.*, *Eur. Phys. J. A*, **50** (2014) 24.
- [4] FANTINA A. F. *et al.*, *Phys. Rev. C*, **93** (2016) 015801.
- [5] CHOMAZ PH. *et al.* (Editors), *Eur. Phys. J. A*, **30** (2006).
- [6] BORDERIE B. and RIVET M.-F., *Prog. Part. Nucl. Phys.*, **61** (2008) 551.
- [7] STRACENER D. W. *et al.*, *Nucl. Instrum. Methods A*, **294** (1990) 485.
- [8] POUTHAS J. *et al.*, *Nucl. Instrum. Methods A*, **357** (1995) 418.
- [9] KWIATKOWSKI K. *et al.*, *Nucl. Instrum. Methods A*, **360** (1995) 571.
- [10] SARANTITES D. G. *et al.*, *Nucl. Instrum. Methods A*, **381** (1996) 418.
- [11] PAGANO A. *et al.*, *Nucl. Phys. A*, **734** (2004) 504.
- [12] WUENSCHEL S. *et al.*, *Nucl. Instrum. Methods A*, **604** (2009) 578.
- [13] BOUGAULT R. *et al.*, *Eur. Phys. J. A*, **50** (2014) 47.
- [14] BARLINI S. *et al.*, *Nucl. Instrum. Methods A*, **600** (2009) 644.
- [15] BARDELLI L. *et al.*, *Nucl. Instrum. Methods A*, **654** (2011) 272.
- [16] FLORES J. L. *et al.*, *Nucl. Instrum. Methods A*, **830** (2016) 287.
- [17] PASTORE G. *et al.*, these Proceedings.
- [18] BONNET E. *et al.*, these Proceedings.
- [19] LACROIX D. *et al.*, *Phys. Rev. C*, **69** (2004) 054604.
- [20] ITOH M. *et al.*, *Phys. Rev. Lett.*, **113** (2014) 102501.
- [21] RADUTA AD. *et al.*, *Phys. Lett. B*, **705** (2011) 65.
- [22] GRENIER F. *et al.*, *Nucl. Phys. A*, **811** (2008) 233.
- [23] POCHODZALLA J. *et al.*, *Phys. Rev. C*, **37** (1987) 1995.
- [24] FRANKLAND J. D. *et al.*, <http://indra.in2p3.fr/KaliVedaDoc>.
- [25] CARBONI S. *et al.*, *Nucl. Instrum. Methods A*, **664** (2012) 251.
- [26] TAN W. P. *et al.*, *Phys. Rev. C*, **69** (2004) 061304.